Preparation and Characterization of the Foam-Stabilizing Properties of Cellulose–Ethyl Cellulose Complexes for Use in Foods

ARTICLE *in* JOURNAL OF AGRICULTURAL AND FOOD CHEMISTRY · NOVEMBER 2011

Impact Factor: 2.91 · DOI: 10.1021/jf203501p · Source: PubMed

5 AUTHORS, INCLUDING:

Kalpana Durga
Leeds Beckett University
3 PUBLICATIONS **72** CITATIONS

SEE PROFILE

Simeon Stoyanov
Unilever R&D, Vlaardingen, the Netherlands
128 PUBLICATIONS **1,347** CITATIONS

SEE PROFILE

Journal of Agricultural and Food Chemistry
Msc: jf203501p

The following graphic will be used for the TOC:

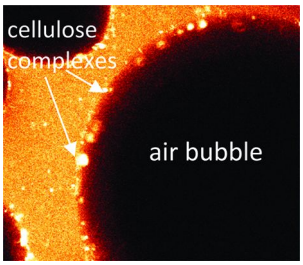

JOURNAL OF AGRICULTURAL AND FOOD CHEMISTRY

Article

pubs.acs.org/JAFC

Preparation and Characterization of the Foam-Stabilizing Properties of Cellulose–Ethyl Cellulose Complexes for Use in Foods

Brent S. Murray,*[,†] Kalpana Durga,[†] Peter W. N. de Groot,[‡] Antonia Kakoulli,[†] and Simeon D. Stoyanov[‡]

[†]Food Colloids Group, School of Food Science and Nutrition, University of Leeds, Leeds LS2 9JT, U.K.

[‡]Unilever R&D Vlaardingen, 3133AT Vlaardingen, The Netherlands

Supporting Information

ABSTRACT: Surface active cellulose particles have been prepared for use as foam stabilizing agents in foods. Various sources of cellulose were broken down by combinations of milling, acid dissolution and treatment with cellulase. The most efficient and simple method was hammer and freezer milling of dry crystalline α-cellulose (Tencel). The resultant Tencel particles were made partially hydrophobic through precipitation of ethyl cellulose (EC) onto them in acetone–water dispersions. The optimum ratio of EC to cellulose and the optimum solids concentration (C_x) at which to form the complexes were 1:1 and $C_x \approx 1$ wt %, respectively. Complexes combined at low concentrations (e.g., $C_x \approx 0.1$ wt %) with caseins or whey proteins gave significant improvements in stability of foams and bubbles to coalescence and disproportionation compared to either component alone. As such, the complexes could be a useful ingredient in improving the quality of various food foams.

KEYWORDS: *cellulose, proteins, foams, coalescence, disproportionation*

INTRODUCTION

Highly stable foams can be produced using surface active particles as the foam stabilizing agents. The stabilization of food foams by particles has been reviewed by Murray and Ettelaie.[1] Binks and Horozov[2] have provided a monograph on the subject of particle-stabilized colloids in general, while Dickinson[3] has more recently reviewed the stabilization of both emulsions and foams by particles in the context of foods. The key feature of particle-stabilized systems is that if the particles have an appropriate size and the correct surface energy or contact angle with the interface, then the energy of desorption per particle can be of the order of several thousand kT (where k = the Boltzmann constant and T = absolute temperature). Such particles are thus effectively irreversibly adsorbed. Although proteins and/or low molecular weight surfactants (LMWS) are exploited in foods to give excellent foamability of aqueous solutions plus good stability to coalescence, proteins and LMWS are generally not good at preventing disproportionation.[4] Surface active particles, on the other hand, can give bubbles that are extremely stable to coalescence *and* disproportionation, through one or a combination of (i) sintering of solid surfaces at the interface; (ii) cross-linking of particles at the interface; (iii) the extreme barrier to particle desorption and therefore resistance to any rearrangement of the interfacial packing. In this way bubbles are not able to shrink once a certain coverage of particles is achieved, even though the fraction of surface actually covered is low (particularly in the case of fibrous particles). Another mechanism by which particles can give apparent high foam stability is through an extreme increase in the viscosity of the bulk aqueous phase via aggregation of the particles, in which the bubbles become trapped.

Although particles may give these advantages in terms of foam stability, they can be disadvantageous in terms of giving relatively low foamability. This is because they are larger entities than molecules of surface active species. Mass transport and adsorption of particles to interfaces may therefore not be rapid enough to stabilize the smallest required bubbles formed during whipping, etc. Particle surface activity at the A–W interface, i.e., hydrophobicity, increases the tendency for particle aggregation in the aqueous phase that further slows down coverage of bubbles by the solid material. In this respect fiberlike particles may have a distinct advantage because even lower surface coverage needs to be reached in order to stabilize the bubbles as the fibers overlap and form a self-supporting network at the interface.[5] On the other hand, the higher is the aspect ratio of the particles, the greater will be their tendency to interlock in the bulk phase, increasing the bulk viscosity and inhibiting incorporation of air in the first place. In addition, interesting questions arise if both proteins and particles happen to be present together, as will almost certainly be the case in most real food products. Proteins will probably adsorb to the particles and change their contact angle and adsorption characteristics. Interfacial coverage is likely to be dominated by the proteins, at least in the early stages of adsorption, since the particles will probably adsorb more slowly due to their higher mass. Whether proteins might be able to displace particles, or vice versa, is not clear, nor whether the two types of components may act synergistically with respect to foaming or foam stability. Competitive adsorption and interactions between model silica particles and cationic LMWS have been investigated elsewhere,[6−8] while competitive adsorption between such silica particles and proteins has been investigated by Kostakis et al.[6]

Received: August 31, 2011
Revised: November 8, 2011
Accepted: November 21, 2011

   dx.doi.org/10.1021/jf203501p | J. Agric.Food Chem. XXXX, XXX, XXX–XXX

There is a need to find surface active particles that are easy and cheap to prepare and that are compatible with food safety and quality. In this study we have focused on particles prepared from cellulose materials[9] that can be regarded as contributing to natural insoluble fiber in foods. Plant or bacterial cellulose can be made hydrophobic by complex formation with suitable additives:[10,11] in this work ethyl cellulose (EC) was used. In order to act as an efficient stabilizer of acceptably small bubbles or emulsion droplets, attempts were made via a variety of techniques and procedures, summarized earlier[12] but detailed here, to reduce the cellulose particle size before complex formation with EC. Since surface active cellulose particles are unlikely to be the sole surface active agent present in real food formulations, we have also investigated the behavior of mixtures of such particles with casein and whey proteins, that are widely exploited in foods for their surface active properties. Stability to both coalescence and disproportionation were investigated in simple rapid tests and more detailed experimental studies.

MATERIALS AND METHODS

Potassium dihydrogen phosphate, disodium phosphate, hydrochloric acid, acetone, sodium hydroxide, sodium acetate trihydrate and glacial acetic acid were of AnalR grade and obtained from Sigma-Aldrich (Gillingham, U.K.). Ethyl cellulose (EC) (product code 02366, 48.0 to 49.5% ethoxyl content) and bovine β-lactoglobulin (BL) (three times crystallized, lyophilized, desiccated, lot no. 21K7079, containing variants A and B) were also obtained from Sigma-Aldrich. Sulfuric acid (98%) and hydrochloric acid (98%) were AnalR grade from Fisher Scientific, U.K. Congo Red and *N*-methylmorpholine *N*-oxide (NMO) were obtained from Acros Organics (Geel, Belgium). Spray-dried sodium caseinate (SC) (>82 wt % dry protein, < 6 wt % moisture, < 6 wt % fat and ash, 0.05 wt % calcium) was supplied by DMV International (Veghel, The Netherlands). Commercial whey protein isolate (BiPro) was obtained from Davisco Foods (Le Sueur, MN, USA) and contained 97.7% protein (on a dry basis), 0.3% fat, 1.9% ash and 4.8% moisture. Water purified by treatment with a Milli-Q apparatus (Millipore, Bedford, U.K.), with a resistivity not less than 18.2 MΩ cm, was used for the preparation of all solutions unless stated otherwise. Aqueous solutions of SC and BL were prepared by dispersing the required amount of protein in buffered Milli-Q water containing 0.02% w/v sodium azide under gentle stirring for 4 h at room temperature. The buffers consisted of 0.05 mol dm^{-3} phosphate + 0.05 mol dm^{-3} NaCl, at pH 6 or pH 7. Cellulase from *Trichoderma viride* (product code: 390742c) was supplied by VWR International.

Three different primary sources of cellulose were used: Tencel (1.7 dtex 3 mm bright Nonwovens H400431, from Lenzing fibres Ltd., Derby, U.K.); microcrystalline cellulose (MCC) from Sigma Aldrich (product code 435244, Brook field RVT viscosity 50 to 150 cps); cellulose extracted from lettuce. Tencel is a pure form of α-cellulose obtained from wood pulp by direct dissolution in *N*-methylmorpholine *N*-oxide. The initial mean length of the Tencel fibers as received was 3 or 12 mm, with a mean width of 20 μm. The MCC was used as received and served as a standard fibrillar cellulose that had already been degraded to finer fibers to some extent. Tencel and MCC are dry solids, and it was therefore of interest to see if a more hydrated form of cellulose from fresh plant tissue would be easier to degrade into finer fibers before complex formation with EC (see below). Lettuce ('Iceberg' variety), purchased from a local supermarket, was chosen as a cheap, readily available material that was rich in cellulose but relatively low in other plant solids. A crude extract of lettuce cellulose was obtained via the method outlined by Fry.[13] Lettuce (300 g) was mixed with 70% ethanol and homogenized via an Ultra-Turrax T25 mixer (Janke & Kunkel, IKA-Labortechnik) for a few seconds until a slurry with a smooth consistency was obtained, i.e., with no particles visible to the naked eye. The slurry was filtered through Whatman No. 1 filter paper and the filtrate removed and dried on a watch-glass in an air oven at 40 °C for 10 h. The dry "alcohol insoluble residue" (AIR) was then cut into small pieces, redispersed in Milli-Q water and mixed via the Ultra-Turrax mixer; then the solids were filtered off and dried as previously. Some samples of AIR were subjected to a low temperature alkali treatment[14] to see if this aided dissolution of the cellulose fibers. In a clean Teflon beaker 1 g of AIR was dispersed in 100 g of 6% NaOH for 1 h at room temperature (20−25 °C) and then cooled to −15 °C for 45 min; then the dispersion was filtered through a Whatman No. 1 filter paper at room temperature and washed four times with Milli-Q water. The dispersion was then dried in an air oven at 40 °C for 10 h. (When redispersed in Milli-Q water, the pH of the dispersion was 7.3, proving that excess alkali had been removed.)

Some cellulose samples were hammer milled 4 times for 2 min, using a C & N eight inch laboratory hammer mill (Christy Turner Ltd., Ipswich,U.K.), with a 1 to 2 min time gap between each milling. Other samples were freezer-milled 3 times for 2.4 min in a SPEX CertiPrep 6750 cryogenic freezer mill (Metuchen, NJ, USA) with a 2 min time gap between each milling stage, after precooling for 12 min. A standard way of chemically degrading cellulose to smaller fragments and fibrils is to treat the material with very concentrated acids.[15] In "short" acid hydrolysis (SAH), 2 g of cellulose solids was dispersed in 100 g of 55 wt % H_2SO_4 and stirred on a Gallenkamp-SS 618 magnetic hot plate stirrer for 6 h, maintaining the temperature at 55 ± 5 °C. After this time the mixture was centrifuged at maximum speed (3000 rpm) in a Minor MSE-676 bench centrifuge (U.K.) until a clear supernatant was obtained, which was then discarded carefully. The sediment of the fibers was redispersed in Milli-Q water and centrifuged again and the supernatant again discarded. This was repeated 3 times. The sediment was then redispersed in acetone and centrifuged and the supernatant discarded as before; this was also repeated 3 times. At the end of the final washing the acid-hydrolyzed cellulose was dried to constant weight in a hot air oven at 40 °C, which also allowed determination of the final yield. In "prolonged" acid hydrolysis (PAH), after heating at 55 ± 5 °C for 6 h, the sample was cooled to room temperature and left stirring for a further 7 days, the container being kept covered with Parafilm. On the seventh day the dispersion was again heated at 55 ± 5 °C for 5 h and then centrifuged, filtered and washed as described above for the SAH. The cellulase treatment used followed the procedure described by Teleman et al.[16] as follows. Acetate buffer was prepared by mixing 1.36 g of sodium acetate trihydrate in 140 mL of distilled water, and the pH was adjusted to 4.0 by using 0.1 M glacial acetic acid. The cellulase enzyme was dissolved in the acetate buffer to give 1 wt % cellulase. Cellulose was added to the cellulase solution to give 1 wt % cellulose, and the mixture was covered and stirred at room temperature for 3 days. After this time the mixture was centrifuged, filtered and washed as described above for the SAH. Finally, some Tencel cellulose samples were dissolved in *N*-methylmorpholine *N*-oxide (NMO) and precipitated in pH 6 buffer. Tencel (0.03 g) was added to 10 g of a 95 wt % aqueous solution of NMO at 50 °C and stirred for 10 min to completely dissolve the cellulose. This solution was then carefully added, one drop at a time, to 40 g of buffer while being stirred in the Ultra-Turrax mixer. This created a fine dispersion of cellulose fibers, which was then filtered and washed as described above for the SAH treatment.

A Nikon Optiphot light transmission microscope was used for some observations of the various cellulose particles obtained by milling, etc. A small quantity of the particles was tapped onto a glass microscope slide and observed in air.

The method used to make the different cellulose particles surface active was similar to that described by Campbell et al.[17] in order to produce surface active shellac fibers. The cellulose particles were dispersed in acetone at 50 °C, and ethyl cellulose (EC) was added. The dispersion was mixed via a magnetic stirrer while an equal volume of pH 6 aqueous buffer was added. EC is insoluble in water and precipitates onto the cellulose as the dilution takes place, giving rise to hydrophobic patches on the particles that make them surface active. The resultant cellulose−ethyl cellulose (C−EC) particles are hereafter referred to as "cellulose complexes". Different weight ratios of cellulose to EC were used, resulting in complexes with different properties, as described below. The dispersion of complexes was diluted with the appropriate volume of buffer for use in subsequent experiments. The

dx.doi.org/10.1021/jf203501p | J. Agric.Food Chem. XXXX, XXX, XXX−XXX

exact nature of the interactions between the EC and the cellulose is not clear. It is assumed that hydrogen bonding takes place between the polysaccharide chains of the EC and the cellulose, although the EC appears to be localized as distinct globules along cellulose fibers.[17] What is clear is that once complex formation has taken place, the EC seems to be irreversibly adsorbed to the cellulose.

Shake Tests of Foam Stability. In a 15 mL Pyrex test tube (internal diameter 1.5 cm) 5 mL of sample was taken and sealed with a plastic stopper. Parafilm was wrapped around the top to prevent any leakage or evaporation of the sample. A 5 mL sample gave 3.8 ± 0.5 cm height of liquid in the tube before shaking. The sample was hand-shaken in the tube for 30 s continuously in an up and down direction. Shake tests were performed with mixtures of C−EC complexes and proteins; the protein and cellulose solids were mixed via a magnetic stirrer for 1 h before samples were taken for the shake test. Immediately after creating the foam, digital pictures were recorded via a Hitachi KP-MIE/K CCD video camera (purchased from Optivision, Yorkshire, U.K.). Foam heights were measured using Image J software. A Leica TCS SP2 confocal laser scanning microscope (CLSM) was used to obtain detailed images of some bubbles and foams from the shake tests. Congo red (0.5 wt %) was used to stain the cellulose particles. Approximately 80 μL of the stained sample was placed into a laboratory-made welled slide[18] filling it completely. A coverslip (0.17 mm thickness) was placed on top of the well, ensuring that there was no air gap trapped between the sample and coverslip. The samples were scanned at 24 °C, using 10× (NA 0.3) or 40× (NA 1.25) oil-immersion objective lenses, approximately 10−20 μm below the level of the coverslip. Images were recorded at a resolution of 1024 × 1024 pixels and processed using the image analysis software Image J.

Measurement of Stability of Foams to Coalescence. The method has been described in detail elsewhere,[19−22] and only brief information is given here. The aqueous phase (typically 50 mL) was carefully added to the coalescence cell, avoiding foaming. Bubbles were formed in the cell by injecting air at a controlled flow rate beneath the surface of the solution, via a 100 mL syringe attached to a long thin capillary. The pressure is then reduced through expansion of a piston in a cylinder connected to the sealed cell via rigid tubing. The method acts as a sort of accelerated, reproducible measure of coalescence stability that is also of direct relevance to processing of foams where pressure variations occur.[19,22] It took 1 to 2 min to form a sufficient number (several hundred) of bubbles, giving a foam within the cell possessing a fairly small, uniform bubble size and even foam height. In the experiments reported here, bubbles were formed at a pressure of 1 bar (i.e., atmospheric pressure) and the pressure was reduced to 1/3 bar in 20 s, 15 min after forming the foam. The bubbles in the three-dimensional foam expand against each other, and the fraction of bubbles coalescing (F_c) is estimated by image analysis of the layer of foam visible near the wall of the cell via Image J software (see below). All the coalescence experiments were conducted with the materials dissolved/dispersed in the pH 6 phosphate buffer + 0.05 M NaCl. In a small number of experiments, the foam was heated before expansion. After foam formation the system was heated in a water bath at 80 °C for 30 min and then removed and allowed to cool to room temperature before the pressure drop was applied in the usual way. Experiments were repeated at least 3 times, and the results presented are based on the mean values of F_c (minimum reproducibility ±0.06).

When the pressure was dropped, all the bubbles expanded and most of the coalescence appeared to occur within the foam. Also, most coalescence occurred during the first few seconds of the 20 s expansion. Although the foams had a fairly uniform bubble size distribution before expansion, the expansion and coalescence disrupted this uniformity. This sometimes made it difficult to distinguish the boundaries of individual bubbles. However, it was possible to count and measure the sizes of the majority (i.e., at least 80%) of bubbles at the cell wall. In this case it is possible to calculate the fraction of coalescence F_c from the mean radius before expansion (R_i), that observed after expansion (R_{ex}) and that expected if no coalescence occurred (R_0). The calculation is as follows.

The number fraction of bubbles coalescing, F_c, may be stated by

$$F_c = (N_i - N_{ex})/N_i = 1 - (N_{ex}/N_i) \quad (1)$$

where N_i = the initial number of bubbles, i.e., before expansion and N_{ex} = the number of bubbles remaining after a certain amount of expansion. Although images were recorded throughout the expansion process, here we just focus on the state of the foam immediately after the expansion has ceased, i.e., at the end of the 20 s expansion. The total volume of the bubbles before expansion (V_i) is simply given by

$$V_i = N_i k {R_i}^3 \quad (2)$$

where $k = 4\pi/3$. R_i can be measured fairly accurately from the images before expansion since the bubbles are fairly monodisperse in size. After expansion, if no bubbles coalesced, the total volume of the bubbles (V_0) would be given by

$$V_0 = N_i k {R_0}^3 \quad (3)$$

where R_0 is the new radius calculated according to Boyle's law for a decrease in pressure from 1 to 1/3 bar, i.e., $3^{1/3}R_i$.

Assuming coalescence occurs only between the bubbles, the volume of the foam bubbles after expansion (V_{ex}) is given by

$$V_{ex} = N_{ex} k {R_{ex}}^3 \quad (4)$$

where R_{ex} is the observed new mean bubble radius and $V_{ex} = V_0$. Thus, equating eqs 3 and 4 and rearranging, it is seen that

$$N_{ex}/N_i = (R_0/R_{ex})^3 \quad (5)$$

and therefore

$$F_c = 1 - (R_0/R_{ex})^3 \quad (6)$$

F_c calculated via eq 6 was used to describe the data, since it was thought that this was more accurate than that based on counting those bubbles that were clearly distinguishable but ignoring the ones that were not. If one takes these values of F_c as representing the overall foam stability, then one is also assuming that all the bubbles in the bulk foam, i.e., those behind those visible at the wall, behave in a similar manner to those observed at the wall. However, this is also the case for methods based on simply counting the bubbles visible, and since the foams starts off uniform and the expansion is uniform as the pressure is lowered, this is probably a fairly good assumption. Only those foams that were very unstable collapsed to give a very nonuniform foam in three dimensions. It should also be noted that previous measurements of F_c on pressure drop with bulk foams correlated very well with analogous coalescence measurements of a single layer of bubbles with a large planar interface, where every single bubble was visible and could be counted.[20,21] In addition, we have also previously noted[19] that F_c due to a pressure drop under a given set of conditions is not very dependent on R_i, providing it does not vary more than a factor of ca. 2 compared to the mean R_i: the initial bubble size in these experiments was certainly at least as reproducible as this. Finally, if F_c was calculated simply on the basis of those bubbles that could be counted, i.e., eq 1, trends were qualitatively similar, but variability in F_c values was greater.

Measurements of Stability of Single Bubbles to Disproportionation. For detailed measurements of bubble shrinkage, i.e., disproportionation, it is impossible to make sense of slow shrinkage of bubbles in three-dimensional foam systems.[23] Instead we have used our previous simple method where bubbles of appropriate size are injected beneath an immobilized planar A−W interface in a special cell,[24] and their size is monitored as a function of time. The bubbles shrink due to the dissolution of gas into the aqueous phase and through the planar interface: the process has been modeled in detail.[23−25] If multiple bubbles are present, their surfaces must be separated from each other by at least 2 bubble diameters in the interface in order to eliminate the influence of the dissolution of one bubble on another. This was achieved by injecting a low number of bubbles and/or deliberately removing some bubbles from the interface

dx.doi.org/10.1021/jf203501p | J. Agric.Food Chem. XXXX, XXX, XXX−XXX

with a pipet, depending upon how many bubbles remained stable on reaching the interface. These restrictions mean that it is difficult to start the experiment with bubbles of a deliberately selected and controlled size.

RESULTS AND DISCUSSION

Effects on Cellulose of Chemical and Physical Treatments Prior to Complex Formation with EC. Table 1 summarizes the effects of various treatments on Tencel fibers of initial length 3 or 12 mm. Typical size ranges are given for at least 100 to 120 particles observed via light microscopy. It is seen that the main effect is to reduce the fiber length rather than their width. Hammer milling seemed to be the most effective in reducing fiber width, as suggested by the appearance of visible fraying of the ends of the fibers as observed under the light microscope. Freezer milling seemed to produce smaller particulates but with a lower aspect ratio (maximum length/maximum width), i.e., less fiberlike. SAH and PAH on their own produced very low yields of material, that were probably mixtures of fibers that were too thin to be visible under the light microscope plus residual material that was coarser than that obtained by milling. EH on its own produced similar results, though the yield was considerably higher than with SAH or PAH. The amorphous regions of cellulose fibers are believed to be attacked first by acid, with some grafting of sulfate groups to the cellulose molecules in the case of sulfuric acid.[26] This aids the dissolution of finer fibrils and molecules. Campbell et al.[17,27] prepared their cellulose in this way before complex formation with hydrophobic materials. However, such acid dissolution is hazardous and quite slow. Cellulase enzymes are similarly believed to attack first the glycosidic bonds in the amorphous regions. It therefore might be expected that acid or enzymatic attack would make the cellulose more susceptible to mechanical breakdown or, conversely, milling might expose more amorphous regions and increase susceptibility to subsequent chemical degradation. However, it is seen that hammer milling and freezer milling prior to SAH did not produce material very different from SAH. The yields from SAH and PAH were too low to allow subsequent HM, but EH followed by SAH produced just enough material to be freezer milled. This produced perhaps the smallest fragments observed, suggesting that this combined sequential approach did indeed aid cellulose fragmentation. However, the overall yield was still low and the particles were of ill-defined shape. As mentioned in the Introduction, it was thought most desirable to produce fiberlike material for foam stabilization. Overall, the combination of HM + FM seemed to be as good as any of the other treatments in terms of yield and particle size reduction. Chemical treatment, prior to HM + FM, or vice versa, did not seem to have any particular advantages, but had the disadvantages of introducing extra steps and lower yields. The MCC that was used in some experiments (see below) as a ready-made source of cellulose particulates had a mean particle length of 20 ± 15 μm with a mean aspect ratio of 1.6 ± 0.5. This material was therefore similar to the HM + FM Tencel.

Table 2 describes the characteristics of the AIR plant cellulose particles after they had been subjected to similar types of treatment as the Tencel. Typical size ranges are given for at least 100 to 120 particles observed via light microscopy. The initial yield of AIR was calculated on the basis of the typical solids content of the lettuce (0.4 wt %) before alcohol extraction. The size of the AIR particles before milling, etc. was already considerably smaller than that of the Tencel after HM or the commercial MCC particles, even though the AIR particles appeared to consist largely of aggregates of even smaller particles. Some of these even smaller particles were also present in a nonaggregated state. FM seemed to have the effect of breaking up the aggregates into the individual particles, which were revealed to be rodlike in shape, with a low aspect ratio and wide size range. FM followed by UM seemed to induce their accumulation back to larger aggregates, and further treatment by SAH also did not seem to bring about any further advantages in terms of producing more separated particles, smaller particles, or particles of higher aspect ratio. The smallest particles were produced by treatment of the AIR with 6% NaOH as described in Materials and Methods, followed by FM. However, by this stage of processing the cellulose particles appeared to have lost any semblance of a fibrillar shape. Overall, FM of the AIR material, particularly in conjunction with the short alkali treatment, seemed to give much smaller cellulose particles than HM and/or FM of the Tencel, but at the expense

Table 1. Summary of Size Reduction of Tencel Fibers Due to Different Treatments

	fiber length		fiber width/μm			
treatment	init/mm	final/μm	init	final	final particle shape	approx yield/%
SAH[a]	3	300–500	10	10	rods	<1
PAH	3	30–40	10	10	rods	<0.1
HM	12	100–270	10	2–10	fibers with split ends	>95
HM + FM	12	2–60	10	2–10	rods or shapeless	>95
HM + FM + SAH	12	10–60	10	2–10	rods or shapeless	<1
EH	3	600	10	10	rods	70–80
EH + SAH + FM	3	7–15	10	2–5	shapeless	<1

[a]Key: SAH = short acid hydrolysis; PAH = prolonged acid hydrolysis; HM = hammer milling; FM = freezer milling; EH = enzyme (cellulase) hydrolysis. Combinations of these treatments were applied in the order given.

Table 2. Summary of Size Reduction Due to Different Treatments of Acid Insoluble Residue (AIR) of Plant Cell Wall Material

treatment	indiv particle dimens/μm	particle shape	aggregate size/μm	approx yield/%
before treatment[a]	length 6, width < 6	short rods	50	35
FM[b]	length 4–60, width 5–50	short rods		100
FM + UM	3–10	mostly aggregates	50–60	100
FM + UM + SAH	2–10	mostly aggregates	25–250	low
NaOH + FM	1–5	almost spherical		80

[a]As part of the initial preparation of the AIR, the cell wall material was subjected to UM; thus all the above materials were subject to this method of mechanical degradation at least once. [b]Key: FM = freezer milling; UM = Ultra-Turrax mixing; SAH = short acid hydrolysis; NaOH = treatment with 6% NaOH. Combinations of these treatments were applied in the order given.

dx.doi.org/10.1021/jf203501p | J. Agric.Food Chem. XXXX, XXX, XXX–XXX

of reducing the aspect ratio of the particles to values even closer to 1.

Effect of Ratio of Cellulose: Ethyl Cellulose on Foaming Properties of the C−EC Complexes. In order to determine the optimum ratio of cellulose to ethyl cellulose (EC) in the production of surface active C−EC complexes, i.e., the ratio that gave maximum foamability and foam stability, the sample of microcrystalline cellulose (MCC) was used. By using the commercial MCC, rather than the different physically and chemically degraded cellulose produced in our own laboratory (as described above), it was hoped to obtain more reproducible results to guide the choice of ratio for use with the latter cellulose materials, which were more variable in their properties. Also, as already stated above, the size and aspect ratio of the MCC particles was also rather similar to that of the Tencel HM + FM cellulose particles, so any effects of differences in particle size and shape would be expected to be minimal. The effect of the total concentration (C_x) of solids in the complexes on foam properties was also investigated. Figure 1 illustrates the relative stability of foams formed in the test tube shake tests for complexes formed by coprecipitation of MCC and EC at ratios of MCC:EC of 2:1, 1:1, and 1:2, at C_x values ranging from 0.25 to 1 wt %. (Different C_x were obtained simply by diluting down the complexes to the desired level with the appropriate aqueous phase.) The time taken for the foam to collapse to a fraction of its initial height can be taken as a crude estimate of foam stability. Foamability (see later) was expressed as the fractional increase in height of the sample, H_R, compared to the initial height of the solution (3.8 cm) before shaking. So in this case the time, t, for H_R to reduce to 0.2 was taken as a measure of foam stability. This is equivalent to 1 cm of foam on top of a 3.8 cm aqueous phase. This was an easier measure to make than the actual height of the foam layer because the boundary between the foam and the underlying aqueous phase was not always obvious because of the turbidity of some of the dispersions.

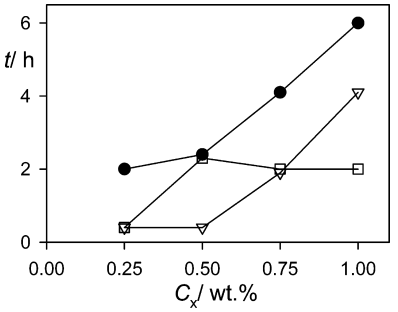

Figure 1. Time (t) for H_R to reduce to 0.2 after shake tests on MCC−EC complexes consisting of different weight ratios of MCC:EC, as a function of total solids concentration (C_x). All tests performed at pH 7 for complexes formed by coprecipitation of 1.5 wt % MCC + 1.5 wt % EC (●); 2 wt % MCC + 1 wt % EC (▽); 1 wt % MCC + 2 wt % EC (□).

Clearly, for the 1:1 and 2:1 MCC:EC complexes, the foam stability increased with increasing C_x, while for the 1:2 MCC:EC complex there was little variation in foam stability (possibly even a slight decrease in stability) with increasing C_x. Overall, the 1:1 MCC−EC complex gave greater stability than the 2:1 MCC−EC complex. These effects are probably due to the fact that, if the MCC:EC ratio is too high, there is not enough EC to confer adequate surface activity to the MCC fibers. Conversely, a low ratio of MCC:EC will mean that there is an excess of EC and the MCC fibers may then become too hydrophobic and aggregate too extensively in the aqueous phase to allow them to adsorb sufficiently rapidly and extensively to the bubble surfaces. In addition, in the latter case, the interface may become predominantly covered with molecules of EC rather than complexes. Shake tests on EC alone showed that the EC gave good foamability, but the foam stability was very poor compared to that of the MCC−EC complexes. This may also explain why there is little dependence on C_x for the 1:2 MCC:EC sample, since across the full range of C_x the interface is essentially dominated by the same species, namely, EC alone. Although they are rudimentary, these tests suggested that there was little to be gained by varying the ratio outside the limits tested and that in fact the 1:1 cellulose:EC ratio should be used.

In Figure 1, the 1:1 MCC:EC complex was formed by coprecipitation of 1.5 wt % MCC with 1.5 wt % EC. The formation of the complexes is a dynamic process, involving diffusion, convection and precipitation of the EC onto the cellulose fibers as they are being mixed. Therefore, it is likely that the exact nature of the complexes formed, i.e., their size and the extent and distribution of the EC coating along the cellulose fibers, will be affected not only by the ratio of cellulose:EC during the precipitation but also by the concentration of cellulose and EC during the coprecipitation. This nature will affect the overall hydrophobicity and surface active properties of the complexes. Therefore, having established that the 1:1 ratio was useful, complexes were formed by coprecipitation at this ratio but at different overall C_x. These different 1:1 complexes were then diluted down to the same C_x and shake tests performed as before. Figure 2 summarizes these results, for 1:1 complexes formed at C_x = 3, 2, 1, and 0.5 wt % solids. Perhaps not surprisingly, it is seen not only that there is a fairly uniform trend for higher stability at higher C_x but also that the higher the initial C_x at which the complexes were formed, the greater the stability, i.e., complexes coprecipitated from 1.5 wt % MCC + 1.5 wt % EC gave the most stable foams. It was noticeable at C_x = 0.75 and 1.0 wt %, dispersions of this complex were fairly viscous, so that at least some of the stabilizing effect might have been due to the trapping of bubbles within a viscous bulk phase. Figure 3 illustrates this aspect in another way, where the initial foam height, relative to the total height of the sample, is plotted

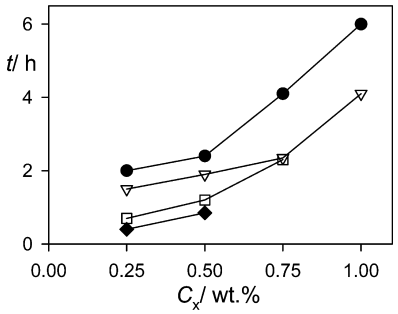

Figure 2. Time (t) for H_R to reduce to 0.2 after shake tests on MCC−EC complexes formed by coprecipitation of the same 1:1 weight ratio of MCC:EC, as a function of total solids concentration (C_x). All tests were performed at pH 7 for complexes formed from 1.5 wt % MCC + 1.5 wt % EC (●); 1 wt % MCC + 1 wt % EC (▽); 0.5 wt % MCC + 0.5 wt % EC (□); 0.25 wt % MCC + 0.25 wt % EC (◆).

dx.doi.org/10.1021/jf203501p | J. Agric.Food Chem. XXXX, XXX, XXX−XXX

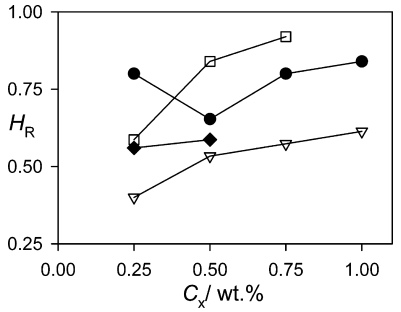

Figure 3. The relative foam height (H_R) not less than 1 min after shaking for MCC−EC complexes formed by coprecipitation of the same 1:1 weight ratio of MCC:EC, as a function of total solids concentration (C_x). All tests were performed at pH 7 for complexes formed from 1.5 wt % MCC + 1.5 wt % EC (●); 1 wt % MCC + 1 wt % EC (▽); 0.5 wt % MCC + 0.5 wt % EC (□); 0.25 wt % MCC + 0.25 wt % EC (◆).

against C_x for the same systems as in Figure 2. The initial foam height is a measure of the *foamability* of the system, and as such it is seen that the complexes formed from 0.5 wt % MCC + 0.5 wt % EC were superior in this sense to both the 1.5 wt % MCC + 1.5 wt % EC and 1.0 wt % MCC + 1.0 wt % EC systems, due to the noticeably higher viscosities of the latter two systems.

High bulk viscosity makes it harder to disperse air into bubbles by shaking and also slows down the mass transport of stabilizers to newly formed bubble surfaces, which therefore coalesce before they are sufficiently covered by a stabilizing material. As is the case with many foaming agents, a compromise often has to be reached between maximum foamability and maximum foam stability. In the case of the C−EC complexes, it was decided that coprecipitation at 0.5 wt % cellulose + 0.5 wt % ethyl cellulose (i.e., C_x = 1 wt %) was a good compromise, and this ratio was used throughout all subsequent work with complexes formed from the different sources of cellulose. The optimum ratio might have been slightly different for each type of cellulose, due to their different specific surface areas or fiber surface properties, for example. However, performing shake tests for different complexes formed from all the samples of cellulose would have been very time-consuming and, furthermore, the differences observed for the MCC systems were not sufficiently large to suggest that the properties of the C−EC complexes were highly sensitive to the C:EC ratio. In addition, the lower C_x value of 1 wt % was more likely to allow practical application of such materials in real food systems.

Effect of the Source of Cellulose on the Foaming Properties of 1:1 Cellulose:Ethyl Cellulose Complexes. C−EC complexes were formed at the 1:1 ratio (i.e., 0.5% C + 0.5 wt % EC), using the method described above, using the other various forms of cellulose produced (see Tables 1 and 2). Table 3 summarizes the foaming properties of these complexes, at C_x = 1 wt %. Tencel subjected to prolonged acid hydrolysis (PAH), or short acid hydrolysis (SAH) in combination with enzyme hydrolysis (EH) and freezer milling (FM), gave complexes that showed reasonable foamability, but not outstanding foam stability: the foams for both systems collapsed within 4 to 6 h. These foam properties were measured at the "natural" pH of the systems, which was pH 2.8. This low pH indicated that, despite the final washing and centrifugation steps of PAH and SAH processing, some residual acid was carried over into the final C−EC complex. When the

Table 3. Foaming Properties of 1 Wt % Dispersions of C−EC Complexes: For Cellulose Obtained via Various Treatments Followed by Complex Formation with EC at a Weight Ratio of 1:1 (i.e. 0.5% C + 0.5 Wt % EC) as Described in the Text

cellulose source, treatment	pH	init H_R[a]	foam collapse time[b]/h
Tencel, PAH[c]	2.8	0.5	6
Tencel, HM	2.5	1.2	5
Tencel, HM + FM	7.0	1.1	320−340
Tencel, EH + SAH + FM	2.8	0.8	4
AIR, FM	6.0	0.8	46−54
AIR, SAH + FM	6.0	0.9	20−24
AIR, NaOH + FM	6.0	0.8	46−54
Tencel, NMO	7.0	0.1	5

[a]The initial relative foam height (H_R) = fractional increase in height of the sample on shaking: the initial height of the solution before shaking (3.8 ± 0.5 cm) not less than 1 min after shaking. [b]The foam collapse time was defined as the time for H_R to reduce to <0.025. [c]Key: PAH = prolonged acid hydrolysis; HM (4×) = hammer milling, 4 times; FM = freezer milling; EH = enzyme (cellulase) hydrolysis; SAH = short acid hydrolysis; AIR = acid insoluble residue obtained from plant cell wall material; NaOH = treatment with 6% NaOH; NMO = Tencel reprecipitated from *N*-methylmorpholine *N*-oxide solution. Combinations of these treatments were applied in the order given.

pH was adjusted to 6 or 7 using the buffers, foaming and foam stability were very poor (results not shown). This may be due to sulfate charging of the cellulose during the acid treatment, which results in large changes in the hydrophobicity and surface activity when the pH or ionic strength is changed. The foaming properties of uncharged complexes would not be expected to be affected by these these changes in solution conditions. On the other hand, when the pH was deliberately lowered (by addition of 0.01 mol dm^{-3} HCl prior to shaking) to a similar value (pH = 2.5) in dispersions of complexes formed from hammer-milled Tencel, the foam stability was similar to that obtained with PAH-Tencel, although the foamability was considerably greater than with the latter .

By far the greatest foam stability was obtained with C−EC complexes formed from hammer-milled + freezer-milled Tencel at neutral pH. Such foams were stable for days on end with hardly any visible changes in their properties. The aqueous phase was clear with a small amount of sediment, indicating that the majority of the complexes had become incorporated into the foam. After 7 days the foam started to slowly collapse, but even after about 10 days there was still some foam remaining. The foamability of these complexes was also good. The only other cellulose material that gave C−EC complexes with comparable foam stability was the AIR material after it had been subjected to the freezer milling, with or without SAH or alkali treatment. In the pH 6 buffer, the AIR material gave foams that were stable for at least 2 days, and the foamability was almost as good as that of the HM + FM Tencel. The aqueous phase was distinctly turbid, however, indicating that a considerable concentration of the AIR−EC complexes remained dispersed in the aqueous phase, unlike with the HM + FM Tencel complexes described above.

C−EC complexes formed using the cellulose prepared by reprecipitation from NMO solution exhibited much lower foamability (initial $H_R \approx 0.1$) than most of the other complexes and also not very good foam stability (foam collapse times of around 5 h). This was despite the fact that these complexes appeared under the microscope to retain the most fibrillar

dx.doi.org/10.1021/jf203501p | J. Agric.Food Chem. XXXX, XXX, XXX−XXX

morphology, characteristic of native cellulose fibrils. Figure 4 compares confocal microcopy images of bubbles stabilized by

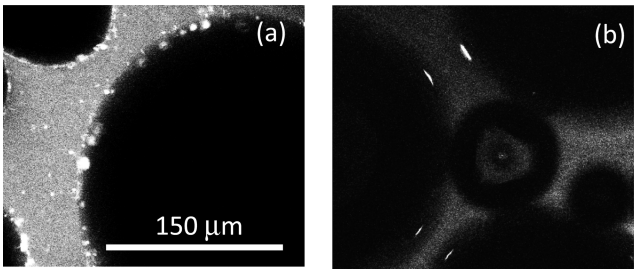

Figure 4. Confocal microcopy images of bubbles stabilized by (a) HM + FM Tencel complexes and (b) NMO−C−EC complexes. Cellulose complex particles appear as bright objects. Bubbles appear as very dark objects against a gray background of aqueous phase.

the HM + FM Tencel complexes with bubbles stabilized by the NMO−C−EC complexes. Congo Red was used to stain the cellulose particles, which appear as bright objects. Bubbles appear as very dark objects against a gray background of aqueous phase. The largest NMO processed C−EC complexes can be seen lying thin and flat at the A−W interface, while the HM + FM Tencel C−EC complexes are obviously present at the interface (and in the bulk aqueous phase) more as rounded aggregates of various sizes.

All in all, the purely physical treatment of the cellulose, i.e., the combination of HM + FM, gave C−EC complexes with the best foaming properties. This was possibly partly due to the retention of some of the fibrillar nature of the cellulose compared to most of the other cellulose materials tested. Moreover, the HM + FM material could be produced in relatively large quantities, which is encouraging for practical applications. Further shake test data (results not shown) revealed that complex formation at higher (2:1) or lower (1:2) ratios of this cellulose to EC did not produce any improvement in foam properties. Therefore, these types of complexes were chosen for more detailed studies of their foam behavior in combination with proteins.

Foaming Properties of 1:1 Cellulose:Ethyl Cellulose Complexes + Proteins. As pointed out in the Introduction, surface active cellulose particles are unlikely to be the sole surface active agent present in real food formulations. In particular, proteins are often present or deliberately added as functional ingredients. Proteins adsorb to most surfaces, and they will therefore compete with the particles at the A−W interface of foams, and they will also adsorb to the surface of the particles themselves, changing the surface active properties of the latter. Sodium caseinate (SC) and whey protein isolate (WPI) were chosen as representative commercial proteins that are used widely in foods for their surface active and gelling properties. Both are mixtures of proteins, but the surface active behavior of SC tends to be dominated by its two principal components: β-casein and α_{s1}-casein. The globular whey proteins tend to be better foaming agents than the caseins,[28] but WPI does contain some low molecular weight contaminants which can significantly affect the overall surface active behavior more than with SC, since the whey proteins are not quite as surface active as SC or such low molecular weight surfactants. For this reason, some experiments were also conducted with pure BL, which is the principal protein of WPI. For the reasons indicated in the above section, C−EC complexes formed from the HM + FM Tencel, with a ratio of C:EC of 1:1, were used in the experiments with proteins.

In the first set of experiments, the same simple shake test used as above was performed for the C−EC + protein mixtures. Protein concentrations (C_p) and complex concentrations (C_x) of 0.1 and 1 wt %, plus salt concentrations of either 0.05 mol dm^{-3} or 0.5 mol dm^{-3} NaCl, were used as those representative of the range of concentrations likely to be encountered in real systems. The pH was fixed at 6 through use of the appropriate phosphate buffer. Figure 5 summarizes the principal findings,

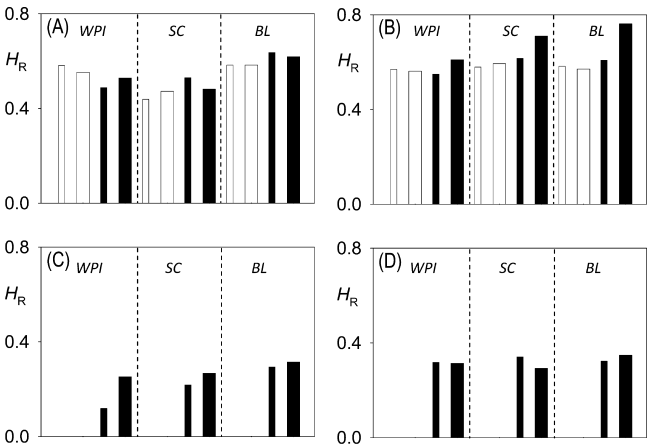

Figure 5. The relative foam height (H_R) for shake tests of Tencel C−EC complexes + whey protein isolate (WPI), sodium caseinate (SC) or β-lactoglobulin (BL): (A) 0.1 wt % protein ± 0.1 wt % C−EC complex after 0.1 h; (B) 1 wt % protein ± 1 wt % C−EC complex after 0.1 h; (C) 0.1 wt % protein ± 0.1 wt % C−EC complex after 24 h; (D) 1 wt % protein ± 1 wt % C−EC complex after 24 h. Open bars = protein only; filled bars = protein + complex. Thin bars = low salt (0.05 mol m^{-3} NaCl); thick bars = high salt (0.5 mol m^{-3} NaCl).

where the relative foam height (H_R) is shown after 0.1 and 24 h, which can be taken as measures of foamability and foam stability, respectively. It is seen that, overall, the addition of the complex to the protein at either 0.1 or 1 wt % at high or low salt concentration has relatively little effect on foamability. (There is, perhaps, a modest increase in foamability through inclusion of the complex). However, the complex is seen to have a dramatic effect on foam stability for all three proteins at both protein concentrations and salt concentrations. In the absence of complexes, H_R = 0 after 24 h for all proteins, whereas significant foam height remained after 24 h in the presence of the complexes. These effects are encouraging in terms of possible practical applications because at high protein concentrations one might expect the extremely high foam stability exhibited by the complexes on their own to be swamped by the presence of protein, or the lower foamability of the complexes to be detrimental to the foamability of the proteins. On the contrary, the two components appear to be complementary to foam stability whereas foamability is not compromised. In order to understand these effects better, more detailed studies of the coalescence and disproportionation characteristics of these mixed foam systems were undertaken, as described below.

Coalescence in Foams Stabilized by 1:1 Cellulose:Ethyl Cellulose Complexes + Proteins. Figure 6a shows F_c versus WPI concentration for systems with and without 0.1 wt % of the C−EC complexes, up to 0.5 wt % WPI. Superimposed on the graph are images of the foams at the end of the 20 s

dx.doi.org/10.1021/jf203501p | J. Agric.Food Chem. XXXX, XXX, XXX−XXX

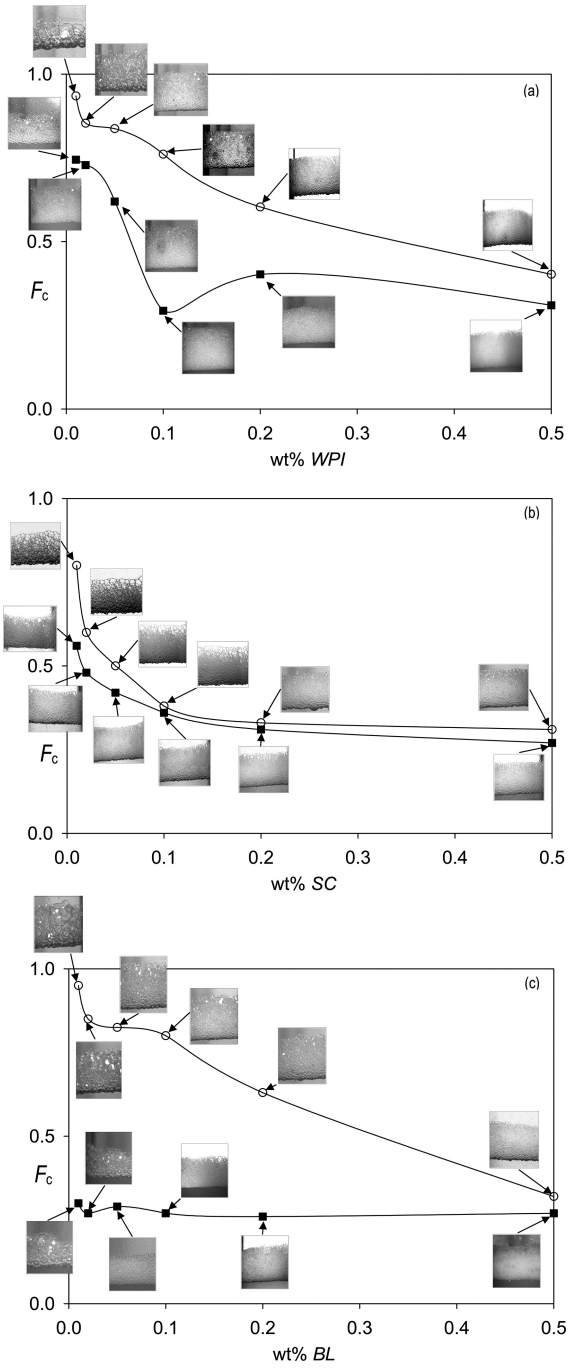

Figure 6. Fraction of bubbles that had coalesced (F_c) by the end of the pressure drop versus concentration of protein at pH 6 + 0.05 M NaCl: in the absence of 0.1 wt % C−EC complexes (○); in the presence of 0.1 wt % C−EC complexes (■) for (a) whey protein isolate (WPI); (b) sodium caseinate (SC); (c) β-lactoglobulin (BL). Superimposed on the plot are images of the foams at the end of the pressure drop for each composition (width of each image 80 ± 2 mm).

expansion (pressure drop). It is clear that the presence of the complexes increases the stability to coalescence (i.e., lowers F_c) considerably, particularly at the intermediate protein concentration (i.e., around 0.1 wt % WPI). In addition, the images show that there were significant qualitative differences in the appearance of the foams. At all bulk protein concentrations (C_p), the foam was more uniform and less coarse after expansion in the presence of the complexes, although this effect was most noticeable at low C_p, where the foam was particularly unstable, especially in the absence of complexes. At high C_p the effect of the complexes was not so great. This was as might be expected, since at high C_p the foaming behavior probably becomes dominated by the protein, which will adsorb more quickly than the complexes. Figures 6b and 6c show the same type of data for SC and BL, respectively. For SC at all C_p the increase in stability on addition of the complexes is not so marked compared to the behavior with WPI, whereas for BL the increase in stability is even greater than with WPI. At C_p < 0.1 wt % BL the value of F_c is very high, i.e., almost all the bubbles coalesce, but in the presence of the complexes F_c is reduced to the lowest values for all 3 systems. The BL system is also noteworthy in that, across all C_p, F_c is essentially the same. The effects with these different proteins can again probably be explained by their different rates of adsorption. SC is known to adsorb more rapidly than globular proteins because the caseins it contains are largely unfolded proteins with a reasonably high degree of hydrophobicity. Consequently, SC adsorption dominates at all C_p whether or not the C−EC complexes are present. On the other hand, the globular whey protein molecules adsorb more slowly because they must unfold to expose their hydrophobic residues in order to adsorb strongly. Because WPI is not a pure protein, lower molecular weight impurities are probably responsible for its behavior being somewhat intermediate between SC and pure BL.

Figure 7 summarizes these differences by replotting the data in a different way for all 3 proteins together. The fraction of

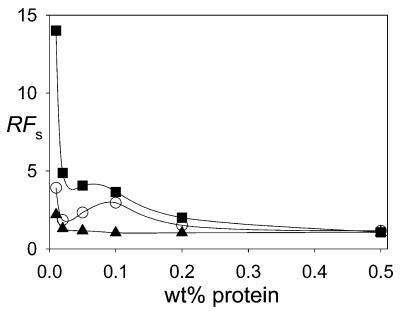

Figure 7. Relative coalescence stability (RF_s) as defined in the text, versus protein concentration, at pH 6 + 0.05 M NaCl, in the presence of 0.1 wt % C−EC complexes for WPI (○); SC (▲); BL (■).

stable bubbles, F_s, may be thought of as a more logical parameter to use when highlighting stability to coalescence, equal to 1 − F_c. In Figure 7 the ratio of F_s in the presence the complexes to that in the absence of the complexes is plotted against C_p for all 3 proteins. The very large increases in stability at low C_p are highlighted, particularly for BL, whereas Figure 6c suggested invariant behavior for BL across all the compositions. It can be seen from the foam images that, in general, the greater the increase in foam stability, the less coarse and more uniform is the foam after the expansion, which is to be expected. However, even when stability is low, there are significant improvements in the uniformity of the foam in the presence of the complexes. For example, compare the images for 0.05 wt % BL with and without complexes in Figure 6c. Thus there appear to be general benefits to foam quality of including this fairly low concentration (0.1 wt %) of cellulose solids, as suggested by the results of the simple test tube shake tests on the mixed systems (Figure 5).

dx.doi.org/10.1021/jf203501p | J. Agric.Food Chem. XXXX, XXX, XXX−XXX

Figure 8 shows the effect of fixing the WPI concentration (C_p = 0.1 wt %) but increasing the concentration of complexes, up

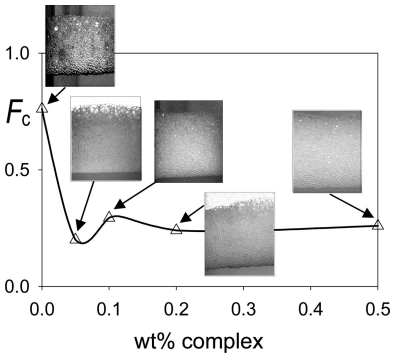

Figure 8. Fraction of bubbles that had coalesced (F_c) by the end of the pressure drop versus concentration of C−EC complexes, at pH 6 + 0.05 M NaCl, in the presence of 0.1 wt % WPI (Δ). Superimposed on the plot are images of the foams at the end of the pressure drop for each composition (width of each image 80 ± 2 mm).

to C_x = 0.5 wt %. Comparison with Figure 6a shows that there is a further lowering of F_c, i.e., increase in stability for C_p = 0.1 wt % + C_x > 0.05 wt % compared to C_x = 0.1 wt % + C_p > 0.5 wt %, but the difference is modest. It has already been noted that at high C_x the systems became significantly more viscous. Because of this, and also because it was thought systems of high cellulose solids were probably unrealistic in terms of practical applications, no further work was done on the other proteins at C_x > 0.1 wt %. In any case the BL system, for example, showed good stability (F_c < 0.3) with C_x = 0.1 wt %. The degree of instability observed is also a function of the rate and extent of the pressure drop, but previous measurements on pure proteins up to quite high concentrations[22] have shown that these pressure drop measurements are quite a severe test of stability to coalescence and almost all systems show F_c > 0.2. Exceptions (i.e., F_c < 0.2) were where the protein or polysaccharide concentration in the aqueous phase was high enough for it to gel.[19,22]

In view of the fact that most practical food systems receive or require a heat treatment step, it was also of interest to see how pasteurization temperatures might affect the coalescence stability. Foams formed from 0.1 or 0.5 wt % WPI, in the presence and absence of 0.5 wt % complexes, were heated to 80 °C as described in Materials and Methods. Table 4 lists the

Table 4. Comparison of Coalescence Stability of Nonheated and Heated WPI + Complex Systems

	F_c[a]			
	no complex		+ 0.5 wt % complex	
wt % WPI	nonheated	heated	nonheated	heated
0.1	0.76	0.53	0.30	0.38
0.5	0.4	0.22	0.31	0.16

[a] F_c = the fraction of bubbles that had coalesced by the end of the pressure drop.

values of F_c for the heated and nonheated systems. It is seen that the heat-processing increased the coalescence stability (i.e., reduced F_c) for all the systems, with or without the complexes, with the exception of 0.1 wt % WPI + 0.5 wt % complex, which was marginally less stable due to heating. The value for the heated 0.5 wt % WPI + 0.5 wt % complex system was particularly low: F_c = 0.16, i.e., 86% of the bubbles were completely stable. Such values are similar to those observed for gelatin at C_p > 0.1 wt %, for example.[22] At 0.5 wt % WPI, C_p is still far too low for bulk protein gelation to occur due to heating, and yet on observation of the foam, very little expansion actually took place as the pressure was lowered. This illustrated the tremendous strengthening effect that the C−EC complexes must have had on either the continuous phase between the bubbles or the interfacial film around them under these conditions. The likely strengthening of the interfacial film will be returned to in the final discussion.

Disproportionation in Foams Stabilized by 1:1 Cellulose:Ethyl Cellulose Complexes + Proteins. Figure

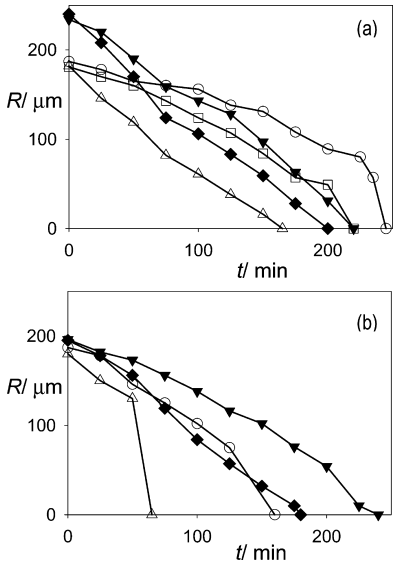

Figure 9. Typical bubble radius (R) versus time (t) for single bubble dissolution beneath the planar A−W interface, in pH 6 buffer + 0.05 M NaCl, for systems consisting of (a) 0.1 wt % C−EC complexes + different wt % concentrations of WPI [0.01 (○); 0.1 (□); 0.2 (◆); 0.5 (▼); 1.0 (△)] and (b) 0.1 wt % WPI + different wt % concentrations of C−EC complexes [0.01 (○); 0.2 (◆); 0.5 (▼); 1.0 (△)].

9a shows typical shrinkage of the bubble radius (R) versus time in the presence of 0.1 wt % C−EC complexes + concentrations of WPI from 0.01 to 1.0 wt %, starting for bubbles with an initial R on injection between 150 and 250 μm. Figure 9b shows similar data, but where the WPI concentration was fixed at 0.1 wt % and the complex concentration was varied between 0.01 and 1.0 wt %. In previous work on different proteins, but without surface active particles present, it was found that is was generally possible to obtain good fits of such R versus time curves to a simple model for dissolution beneath a planar interface. The model solved the gas diffusion equations for changing bubble size versus time, while incorporating an enhanced resistance to shrinkage through a fixed value of the dilatational elasticity (ε), when necessary, to improve the fit. The values of ε obtained were generally independent of the starting radius in the experiment. For the systems investigated here, it is seen that, with the possible exceptions of the systems with very low C_x, the R versus t plots were not smooth, nor did they have the characteristic downward curve typical of the results for systems with protein alone, and it was not possible to

dx.doi.org/10.1021/jf203501p | J. Agric.Food Chem. XXXX, XXX, XXX−XXX

obtain good fits to the data and quantify shrinkage behavior of the different systems. Perhaps this was to be expected, given the significantly different packing of particles + protein at the A−W interface that might occur as the bubbles shrink, compared to a protein film on its own.

Because of the difficulty of controlling the initial bubble radius on injection, it is difficult to compare the data in the raw R versus t plots and discern any meaningful trends in the resistance to shrinkage as a function of C_p or C_x. Figure 10

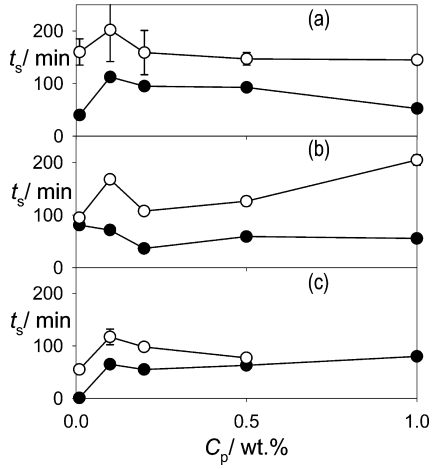

Figure 10. Average shrinkage time (t_s) of bubbles beneath the planar A−W interface measured from an initial radius of 150 μm, in pH 6 buffer + 0.05 M NaCl, for systems consisting of different wt % protein concentrations (C_p) with (○) and without (●) 0.1 wt % C−EC complexes for proteins WPI (a); SC (b) and BL (c). The error bars represent the standard deviations about the mean values.

provides a more useful way of comparing the data where the average shrinkage time, t_s, is reported, defined as equal to the time from when the measured radius equals 150 μm to the time when the bubble has dissolved completely, irrespective of the actual starting radius. In this case "dissolved completely" means that the bubble was no longer clearly visible because it had shrunk to a size that was less than the optical resolution of the microscope (ca. 3 μm). Experiments were repeated at least 2 times, and the minimum reproducibility in these mean t_s values was typically ±10 min. Figure 10 compares t_s data for WPI, SC and BL at different protein concentrations, both in the presence and in the absence of 0.1 wt % C−EC complexes. There are no clear trends as a function of C_p and no clear differences between the different proteins, but it is clear that in all cases t_s was increased considerably in the presence of the complexes, i.e., the systems were more stable to disproportionation.

Although the overall average shrinkage time (t_s) as defined above is useful, it takes no account of the changing rate of shrinkage which is obvious from the plots of the raw data (e.g., Figures 9a and 9b). An attempt was therefore made to summarize the different shrinkage rates by fitting the R versus time data from R = 150 μm over the following 60 min to a straight line, and to use the gradient of this line (dR/dt) as a measure of the shrinkage rate at this stage of the bubble dissolution. Figure 11 shows average values of $-dR/dt$ for WPI, SC and BL for C_p varying between 0.01 and 1 wt %, with and without 0.1 wt % C−EC complexes. The standard deviation for each data point is not given, but it was typically not greater than ±0.4 μm min^{-1}. Within experimental error, only at the lowest C_p can it be said that there were significant differences between

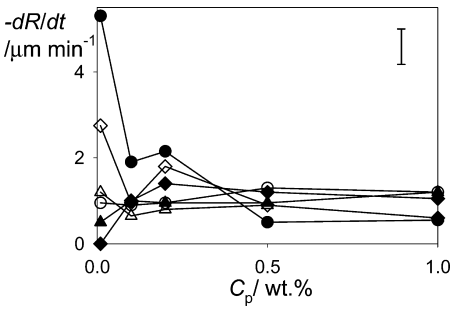

Figure 11. Average rate of shrinkage of radius ($-dR/dt$) of bubbles beneath the planar A−W interface measured from an initial radius of 150 μm for 60 min in pH 6 buffer + 0.05 M NaCl, for systems consisting of different wt % protein concentrations (C_p) with (open symbols) and without (filled symbols) 0.1 wt % C−EC complexes for proteins WPI (○, ●); SC (△, ▲) and BL (◇, ◆).

the different systems: most notably WPI on its own gave a significantly faster shrinkage rate. Since the shrinkage rates as defined above were not very different, this means that the clear differences in shrinkage *time* described in Figure 10 must be attributable to differences in the later stages of bubble shrinkage. Again this might be expected if the C−EC particles only start to exert their influence when the bubbles have shrunk significantly enough to force the C−EC particles to start to pack together tightly at the interface. Figure 12 illustrates this

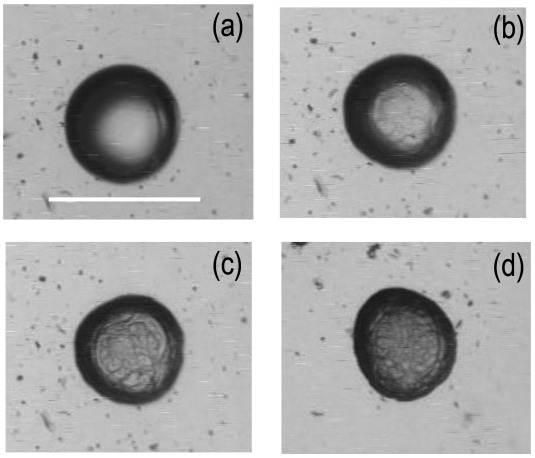

Figure 12. Images of a bubble shrinking in a system of 1 wt % BL + 0.1 wt % C−EC complexes in pH 6 buffer + 0.05 M NaCl at different times since reaching the planar A−W interface: 2 min (a); 100 min (b); 175 min (c); 300 min (d). The scale in all the images is indicated by the size bar in panel a = 300 μm.

for 1 wt % BL + 0.1 wt % complexes, where at long enough times the surface of the bubbles takes on a distinctly wrinkled appearance and the bubbles can become nonspherical, indicating an extremely stiff interfacial film resistant to further shrinkage. Such behavior was rarely observed for WPI or SC + complexes at equivalent C_p, but has been seen at high C_x (1 wt %) in the absence of proteins.

Conclusions. It has been shown that surface active cellulose particles can be fairly easily prepared through a combination of simple mechanical processing of fibrous cellulose plus minimal chemical processing via addition of ethyl cellulose. Such processes could probably be scaled up easily to provide enough material for practical usage. The

dx.doi.org/10.1021/jf203501p | J. Agric.Food Chem. XXXX, XXX, XXX−XXX

complexes formed between the cellulose and ethyl cellulose show good foam stabilizing properties and moderate foamability when used on their own. The balance of foamability and foam stability depends upon the ratio of cellulose to ethyl cellulose, and in practice it seems that a 1:1 ratio is optimum. However, when the complexes are combined with proteins as foaming agents, there are significant synergistic effects in that both foam formation and foam stability can be significantly greater than with complexes or proteins on their own. The degree of benefit depends on the relative concentration of protein (C_p) and complexes (C_x): at high C_p:C_x ratios the benefits seem to be curtailed. This is probably due to the faster adsorption and higher mobility of proteins compared to the C−EC particles, so that at high C_p:C_x the proteins dominate the behavior. Most benefits are obtained at approximately equal concentrations of proteins and complexes. Most notable is the increase in stability to coalescence, as tested by stability to coalescence induced by applying a pressure drop, while the increase in stability to disproportionation, i.e., bubble shrinkage, is significant but not so marked as with coalescence stability.

It has recently been shown[12] that the surface shear viscosity of the A−W interface in the presence of whey protein isolate, sodium caseinate and pure β-lactoglobulin can be massively increased in the presence of such C−EC particles, whereas the complex dilatational modulus is only moderated affected. This probably explains the considerable increase in coalescence stability obtained with the mixtures of proteins and complexes, while the decrease in disproportionation rates is not quite as significant. Nevertheless, this work indicates that significant improvements in foam quality and stability can be obtained by including just a low concentration (e.g., 0.1 wt %) of these insoluble surface active particles, based on cellulose and ethyl cellulose, that could be used in real foodstuffs.

■ ASSOCIATED CONTENT

Supporting Information

Full size versions of Figures 6a−c and Figure 8, where the differences in the images of the foams may be more clear. This material is available free of charge via the Internet at http://pubs.acs.org.

■ AUTHOR INFORMATION

Corresponding Author

*School of Food Science & Nutrition, The University of Leeds. Leeds LS2 9JT, U.K. Tel: +44 (0) 113 343 2962. Fax: +44 (0) 113 343 2982. E-mail: b.s.murray@leeds.ac.uk.

Funding

K.D. gratefully acknowledges support from Unilever and EPSRC through Industrial CASE award No. 05000846.

■ REFERENCES

(1) Murray, B. S.; Ettelaie, R. Foam stability: proteins and nanoparticles. *Curr. Opin. Colloid Interface Sci.* **2004**, *9*, 314−320.

(2) Binks, B. P.; Horozov, T. S. *Colloidal particles at liquid interfaces*; Cambridge University Press: Cambridge, U.K., 2006.

(3) Dickinson, E. Food emulsions and foams: stabilization by particles. *Curr. Opin. Colloid Interface Sci.* **2010**, *15*, 40−49.

(4) Murray, B. S. Stabilization of bubbles and foams. *Curr. Opin. Colloid Interface Sci.* **2007**, *12*, 232−241.

(5) Alargova, R. G.; Warhadpande, D. S.; Paunov, V. N.; Velev, O. D. Foam superstabilization by polymer microrods. *Langmuir* **2004**, *20*, 10371−10374.

(6) Kostakis, T.; Ettelaie, R.; Murray, B. S. Enhancement of stability of bubbles to disproportionation using hydrophilic silica particles mixed with surfactants or proteins. In *Food colloids: self-assembly and material science*; Dickinson, E., Leser, M., Eds.; Royal Society of Chemistry: Cambridge, U.K., 2007; pp 357−368.

(7) Binks, B. P.; Kirkland, M.; Rodrigues, J. A. Origin of stabilisation of aqueous foams in nanoparticle-surfactant mixtures. *Soft Matter* **2008**, *4*, 2373−2382.

(8) Cui, Z.-G.; Yang, L.-L.; Cui, Y.-Z.; Binks, B. P. Effects of surfactant structure on the phase inversion of emulsions stabilized by mixtures of silica nanoparticles and cationic surfactant. *Langmuir* **2010**, *26*, 4717−4724.

(9) Holt, B. L.; Stoyanov, S. D.; Pelan, E.; Paunov, V. N. Novel anisotropic materials from functionalised colloidal cellulose and cellulose derivatives. *J. Mater. Chem.* **2010**, *20*, 10058−10070.

(10) Andresen, M.; Stenius, P. Water-in-oil emulsions stabilized by hydrophobized microfibrillated cellulose. *J. Dispersion Sci. Technol.* **2007**, *28*, 837−44.

(11) Wege, H. A.; Kim, S.; Paunov, V. N.; Zhong, Q.; Velev, O. D. Long-term stabilization of foams and emulsions with in situ formed microparticles from hydrophobic cellulose. *Langmuir* **2008**, *24*, 9245−53.

(12) Murray, B. S.; Durga, K.; Yusoff, A.; Stoyanov, S. D. Stabilization of foams and emulsions by mixtures of surface active food-grade particles and proteins. *Food Hydrocolloids* **2011**, *25*, 627−638.

(13) Fry, S. C. *The growing plant cell wall: chemical and metabolic analysis*; Longman: New York, 1988.

(14) Wang, Y.; Deng, Y. The kinetics of cellulose dissolution in sodium hydroxide solution at low temperatures. *Biotechnol. Bioeng.* **2009**, *102*, 1398−1405.

(15) Liebert, T. Innovative concepts for the shaping and modification of cellulose. *Macromol. Symp.* **2008**, *262*, 28−38.

(16) Teleman, A.; Harjunpää, V.; Koivula, A.; Ruohonen, L.; Teeri, T. T.; Teleman, O.; Drakenberg, T. Cello-oligosaccharide hydrolysis by cellobiohydrolase II from *Trichoderma Reesei*. *Eur. J. Biochem.* **2004**, *240*, 584−591.

(17) Campbell, A. L.; Holt, B. L.; Stoyanov, S. D.; Paunov, V. N. Scalable fabrication of anisotropic micro-rods from food-grade materials using an in shear flow dispersion-solvent attrition technique. *J. Mater. Chem.* **2008**, *18*, 4074−4078.

(18) Moschakis, T.; Murray, B. S.; Dickinson, E. Microstructural evolution of viscoelastic emulsions stabilised by sodium caseinate and xanthan gum. *J. Colloid Interface Sci.* **2005**, *284*, 714−728.

(19) Murray, B. S.; Dickinson, E.; Gransard, C.; Söderberg, I. Effect of thickeners on the coalescence of protein-stabilized air bubbles undergoing a pressure drop. *Food Hydrocolloids* **2006**, *20*, 114−123.

(20) Murray, B. S.; Cox, A.; Dickinson, E.; Nelson, P. V.; Wang, Y. Coalescence of expanding bubbles: effects of protein type and included oil droplets. In *Food colloids: self-assembly and material science*; Dickinson, E., Leser, M., Eds.; Royal Society of Chemistry: Cambridge, U.K., 2007; pp 369−382.

(21) Murray, B. S.; Dickinson, E.; Wang, Y. Bubble stability in the presence of oil emulsion droplets: influence of surface shear versus dilatational rheology. *Food Hydrocolloids* **2009**, *23*, 1198−1208.

(22) Murray, B. S.; Dickinson, E.; Lau, C. K.; Schmidt, E. Coalescence stability of protein-stabilized bubbles when undergoing expansion at a simultaneously expanding planar air-water interface. *Langmuir* **2005**, *21*, 4622−4630.

(23) Ettelaie, R.; Dickinson, E.; Du, Z.; Murray, B. S. Disproportionation of clustered protein-stabilized bubbles at planar air-water interfaces. *J. Colloid Interface Sci.* **2003**, *263*, 47−58.

(24) Dickinson, E.; Ettelaie, R.; Murray, B. S.; Du, Z. Kinetics of disproportionation of air bubbles beneath a planar air-water interface stabilised by food proteins. *J. Colloid Interface Sci.* **2002**, *252*, 202−213.

(25) Dickinson, E.; Ettelaie, R.; Kostakis, T.; Murray, B. S. Factors controlling the formation and stability of air bubbles stabilized by partially hydrophobic silica nanoparticles. *Langmuir* **2004**, *20*, 8517−8525.

981 (26) Marchessault, R. H.; Morehead, F. F.; Walter, N. M. Liquid
982 crystal systems from fibrillar polyssachharides. *Nature* **1959**, *184*, 632−
983 633.
984 (27) Campbell, A. L.; Stoyanov, S. D.; Paunov, V. N. Fabrication of
985 functional anisotropic food-grade micro-rods with microparticle
986 inclusions with potential application for enhanced stability of food
987 foams. *Soft Matter* **2009**, *5*, 1019−1023.
988 (28) Dickinson, E. *An Introduction to Food Colloids*; Oxford
989 University Press: Oxford, U.K., 1992.